

# Coil-Globule Transition of Poly(*N*-isopropylacrylamide). A Study of Surfactant Effects by Light Scattering

M. Meewes, J. Rička,\* M. de Silva, R. Nyffenegger, and Th. Binkert

*Institute of Applied Physics, University of Berne, 3012 Berne, Switzerland*

*Received March 12, 1991; Revised Manuscript Received June 24, 1991*

**ABSTRACT:** The phase behavior of a fractionated high molecular weight sample of poly(*N*-isopropylacrylamide) in dilute aqueous solution containing a surfactant, sodium dodecyl sulfate (SDS), is studied with temperature and surfactant concentration as independent variables. Static and dynamic light scattering are used as methods of investigation. Without surfactant, the polymer exhibits a lower critical solution temperature (LCST) of 34 °C, above which it precipitates. At SDS concentrations of only 250 mg/L, aggregation is completely prevented (intermolecular solubilization) and the behavior of isolated polymer molecules can be studied in the whole temperature range: Upon heating, the polymer undergoes a coil-to-globule phase transition with a volume reduction by a factor of more than 300. The transition temperature depends on the surfactant concentration. It is first constant and equal to the LCST, but begins to increase above 300 mg/L surfactant. Therefore when increasing the surfactant concentration at constant temperatures above the LCST, we cross the phase boundary and observe intramolecular solubilization, i.e., a surfactant-induced globule-to-coil transition. Below the LCST, the surfactant causes an expansion of the polymer coils also setting on at 300 mg/L.

## Introduction

The properties of macromolecules in solutions depend strongly on temperature. Macroscopically, one observes changes in the solubility behavior: Generally, an increase of temperature leads to an increase in solubility, although for certain synthetic polymers, the opposite behavior is also known.<sup>1</sup> On a microscopic scale, the polymer molecules may undergo drastic conformational changes. One example for such a conformational change (well-known, but still subject to discussion) is the coil-globule transition of polystyrene in cyclohexane;<sup>2,3</sup> another one is the thermal denaturation of proteins. Such effects on the polymer solution properties can be influenced by the addition of surfactants: Because of their technological and biological significance, the solubilization of otherwise insoluble polymer by surfactants and the surfactant-induced helix-coil transition of proteins have received much attention.<sup>4,5</sup> In a recent letter,<sup>6</sup> we have reported a system which incorporates in an intriguing way all four aspects outlined above: we observe changes in solubility as well as conformational changes, both influenced by temperature and surfactant. This system is poly(*N*-isopropylacrylamide) (poly(NIPAM)) in dilute aqueous solutions containing small amounts of sodium dodecyl sulfate (SDS).

Poly(NIPAM) in aqueous solution exhibits a lower critical solution temperature (LCST) of ca. 34 °C (values between 31 and 35 °C have been reported). This has been known for a long time; a first systematic study was conducted by Heskins and Guillet in 1968.<sup>7</sup> A renewed interest in this thermoreversible phase transition, triggered by its potential technological applicability and by its relevance to the problem of collapsing polymer chains (coil-globule transition) has lately resulted in a number of publications: Many applications such as thermosensitive sun shadings, adsorbents, drug-release devices, thermally induced enzyme immobilization, and immunoassay procedures have been proposed or patented.<sup>8-12</sup> The fundamental polymer research concentrated first on poly(NIPAM) gels,<sup>13</sup> observing a collapse of the polymer network. Subsequent investigations of the conformation of isolated poly(NIPAM) molecules, however, have been hampered by the fact that at the temperatures of interest, viz., in the vicinity and above the LCST, intermolecular

aggregation occurs even at extremely low concentrations.<sup>6,14</sup> Nevertheless, studies based on fluorescence methods<sup>15,16</sup> and light scattering<sup>14,17-19</sup> have given evidence for a transition from the extended coil to the collapsed globule state at the transition temperature. Our group has conducted a series of experiments using time-resolved fluorescence to investigate the local mobility of labeled polymer segments; the results of these experiments also corroborate this picture of collapsing polymer coils.<sup>20</sup> Schild and Tirrell<sup>21</sup> have studied mixtures of poly(NIPAM) and various *n*-alkyl sulfates using fluorimetric and turbidimetric methods. They found that very small amounts of SDS (<5 mg/L) are sufficient to clarify the solutions above the LCST and that some surfactants shift the transition temperature to a value  $T_C$  which is higher than the LCST of surfactant-free solutions. (The hydrocarbon tails of the amphiphiles must be sufficiently long to allow the formation of micelles.) Furthermore, they determined a critical association concentration (CAC) of 230 mg/L for the binding of surfactant molecules to the polymer. (The CAC is thus much lower than the critical micellization concentration (CMC) of SDS in water, which amounts to 2.3 g/L.) The authors conclude that in the vicinity of the CAC, the surfactant molecules cooperatively bind to the polymer chains in the form of adsorbed micelles.

In our previous study,<sup>6</sup> we investigated the microscopic features of this solubilization of poly(NIPAM) by SDS. At fixed temperatures above the LCST, the solubilization proceeds in two distinct steps: At low surfactant concentrations, *intermolecular solubilization* prevents aggregation, allowing the investigation of a stable solution of isolated polymer molecules in the globule state. Increasing surfactant concentration results in *intramolecular solubilization*, i.e., the conformational transition from a compact globule to an expanded coil. This intramolecular solubilization is consistent with the elevation of the transition temperature of the SDS-poly(NIPAM) solutions as compared to the surfactant-free system. The object of our first study was a sample of poly(NIPAM) with a relatively broad weight distribution that was investigated mainly by means of dynamic (quasielastic) light scattering (QLS) at one fixed scattering angle. In this paper, we continue our work using more refined

methods of investigation, viz., simultaneous dynamic and static light scattering, both angle dependent. The sample is also better defined, with high molecular weight and a narrow weight distribution. We are thus in a position to monitor the conformational changes of the polymer molecules more closely and more precisely. Furthermore, by comparing the data from our two investigations, we are able to assess a possible dependency of the phase behavior on molecular weight and polydispersity. The results will be discussed in terms of the coil-globule transition and adsorption effects of surfactant molecules to the polymer.

### Data Analysis

**Static Light Scattering.** The static light scattering of a particle suspension is commonly characterized by the Rayleigh ratio  $R_\theta$ , i.e., by the differential scattering cross section per unit volume of suspension at scattering angle  $\theta$ . The Rayleigh ratio can be calculated from experimentally accessible quantities as<sup>22</sup>

$$R_\theta = \frac{I_s(\theta)}{I_t(\theta)} \left( \frac{n}{n_t} \right)^2 R_{\theta,t} \quad (1)$$

where  $I_s(\theta)$  is the excess scattering intensity of the solute and  $I_t$  the scattering intensity of a standard (usually toluene) with a known Rayleigh ratio  $R_{\theta,t}$ . The square ratio of the refractive indices of solvent and scattering standard  $(n/n_t)^2$  accounts for the corrections of solid angle and scattering volume. For dilute solutions satisfying the Rayleigh-Debye approximation, the theoretical expression for  $R_\theta$  can be written as the sum of two terms<sup>23</sup>

$$R_\theta = C[P(q) + Q(q,c)c] \quad (2)$$

With  $q$ , we denote the absolute value of the scattering vector ( $q = 4\pi n/\lambda \sin(\theta/2)$ ,  $\lambda$  being the incident wavelength in vacuo), and  $c$  is the weight concentration of the solute. In the simple case of optically uniformity (e.g., homopolymers) and for vertically polarized incident light, the constant  $C$  is given by

$$C = \frac{[2\pi n(dn/dc)]^2}{\lambda^4 N_A} c M_w = K c M_w \quad (3)$$

where  $(dn/dc)$ ,  $N_A$ , and  $M_w$  are the refractive index increment of the solute, Avogadro's constant, and the weight-average molecular weight of the solute. In the first (self) term of eq 2, the particle scattering factor  $P(q)$  describes the geometrical structure of the solute particles, whereas the second (distinct) term  $Q(q,c)$  is also affected by interactions between the particles. For small  $q$  and  $c$ ,  $Q(q,c)$  can be expressed in terms of the second virial coefficient  $A_2$ ; viz.,  $Q(q,c)_{q,c \rightarrow 0} = -2A_2$ .<sup>23</sup> For Gaussian coils in the dilute regime, the influence of the distinct term on the angle dependency of the scattering intensity is minimized by the fact that  $Q(q,c) \approx -2A_2 P(q)$ , leading to Zimm's famous formula<sup>24</sup>

$$\frac{K_c}{R_\theta} = \frac{1}{M_w P(q)} + 2A_2 c \quad (4)$$

The magnitude of  $A_2$  determines the concentration range in which the second term in (4) or (2) may be neglected. For our experiments, we chose a polymer concentration where this contribution is negligible (see data in section Characterization). For Gaussian coils,  $P(q)$  is given by

the well-known expression of Debye<sup>25</sup>

$$P(q) = \frac{2}{(R_g q)^4} [\exp[-(R_g q)^2] - 1 + (R_g q)^2] \quad (5)$$

$R_g$  being the root mean square radius of gyration of the coils. For expanded coils in good solvents, this expression is strictly valid for the description of the angular variation of the scattering intensity only at small and intermediate scattering angles, because excluded volume effects manifest themselves at large scattering angles<sup>26</sup> (see also Figure 4). We therefore use only intensity data from angles  $\leq 70^\circ$  for the determination of  $R_{\theta=0}$  and  $R_g$  from eq 4 (neglecting the contributions of the second term) in conjunction with (5). For collapsed globules,  $(R_g q)^2 \ll 1$  in the whole range of scattering angles. In this limit

$$P(\theta) \approx 1 - 1/3 (R_g q)^2 \quad (6)$$

independent of particle structure.<sup>27</sup> The solubilized, isolated globules can be viewed as nonattracting hard spheres. For these, the distinct term can be written as  $8V_{\text{sphere}} N_A / M_w c$ , which in our experiments was  $\leq 0.02$  and likewise neglected in the determination of  $R_{\theta=0}$  and  $R_g$  in the globule state using eq 4 and 6. Aggregation of the polymer molecules caused by attractive interactions would result in an enhancement of forward scattering ( $R_{\theta=0}$ ) above the value given by the molecular weight of the polymer. We therefore use  $R_{\theta=0}$  to monitor a possible formation of interpolymeric aggregates above the LCST.

**Dynamic Light Scattering.** For an ideal solution of uniform, noninteracting, rigid, isotropic scatterers, the normalized intensity time correlation function  $g^{(2)}(\tau) = \langle I(0) I(\tau) \rangle / \langle I \rangle^2$  obeys the relation<sup>28</sup>

$$g^{(2)}(\tau) = 1 + A e^{-\gamma \tau} \quad (7)$$

$A$  is an apparatus-dependent coherence factor,  $\tau$  the delay time, and  $\gamma$  the relaxation rate  $2q^2 D$ ,  $D$  being the translational diffusion coefficient of the solute. For a real system of polydisperse, interacting, flexible polymer chains,  $g^{(2)}(\tau)$  is characterized by a superposition of exponentials with the distribution  $f(\gamma)$  of relaxation rates:

$$g^{(2)}(\tau) = 1 + A \left| \int f(\gamma) e^{-\gamma \tau} d\gamma \right|^2 \quad (8)$$

The technique we use for data analysis is the standard cumulant method.<sup>28</sup> Besides the quantity  $A$ , we calculate the first three cumulants corresponding to the mean relaxation rate  $\langle \gamma \rangle$ , the variance  $\langle \Delta \gamma^2 \rangle$ , and a measure of the skewness of  $f(\gamma)$  from a four-parameter fit of the QLS data. In the limit of small scattering angles and dilute solutions<sup>22</sup>

$$\langle \gamma \rangle / q^2 = \langle D \rangle_z (1 + B q^2) (1 + k_D c) \quad (9)$$

where  $\langle D \rangle_z$  is the  $z$ -average translational diffusion coefficient,  $B$  a constant depending on the size, structure, and polydispersity of the polymer, and  $k_D$  a constant describing the concentration dependence of  $\langle D \rangle_z$ . For our samples,  $k_D c \leq 0.025$  (see section Characterization) and was neglected in the determination of  $\langle D \rangle_z$ . The term  $B q^2$ , however, is of the order of unity in the experimentally accessible angle range, and we determine  $\langle D \rangle_z$  by extrapolation of angle-dependent QLS data to zero scattering angle. The equivalent hydrodynamic radius  $R_h$  is calculated from  $\langle D \rangle_z$  using the Einstein relation and Stokes' formula for the friction of a sphere in a solvent with

viscosity  $\eta$ :

$$R_h = \frac{kT}{6\pi\eta \langle D \rangle_z} \quad (10)$$

The variance  $\langle \Delta\gamma^2 \rangle$  obtained from the second cumulant is a measure for the polydispersity and internal motions of the polymer chains. For collapsed, rigid globules, where the flexibility effects are absent,  $\langle \Delta\gamma^2 \rangle = q^4 \langle \Delta D^2 \rangle_z$ . We use this fact to determine the polydispersity of the sample: For globules, the diffusion coefficient is related to the molecular weight by  $D(M) \propto M^{-1/3}$ . We assume that the molecular weight is distributed according to the  $\Gamma$  distribution (Schultz distribution):

$$f(M) = \frac{1}{\lambda!} \left[ \frac{\lambda + 1}{\langle M \rangle} \right]^{\lambda+1} M^\lambda \exp \left[ -\frac{(\lambda + 1)M}{\langle M \rangle} \right] \quad (11)$$

The parameter  $\lambda$  is a measure of polydispersity ( $\lambda = \infty$  denotes a monodisperse system). Using (11) and (8), one can obtain an expression for the relative variance in terms of  $\lambda$ :

$$\frac{\langle \Delta\gamma^2 \rangle}{\langle \gamma^2 \rangle} = \frac{\langle \Delta D^2(M) \rangle_z}{\langle D(M) \rangle_z^2} = \frac{\Gamma(\lambda+1+4/3)\Gamma(\lambda+3)}{\Gamma(\lambda+1+5/3)^2} - 1 \quad (12)$$

This equation can be numerically solved for  $\lambda$ , and the index of polymer polydispersity  $M_w/M_n$  is obtained through the relation  $M_w/M_n = (\lambda + 2)/(\lambda + 1)$ .

## Experimental Section

**Synthesis and Fractionation.** The monomer, NIPAM, was purified by crystallization from a 50 wt % benzene-hexane mixture. The polymer was synthesized by the radical polymerization method of Kulicke and Klein,<sup>29</sup> designed to obtain high molecular weight while minimizing the branching: At room temperature, 60 mg of  $H_2O_2$  was added as initiator to an oxygen-free solution of 5 g of NIPAM and 95 g of deionized water. Polymerization was conducted at 27 °C for 10 h, resulting in a polymer yield of 60%. The polymerization product was separated from the monomer by repeated precipitation through heating in aqueous solution, vacuum-dried, dissolved in methanol, and fractionated into seven fractions by means of a Knauer HPLC apparatus, controlled pore glass beads with a pore size of 200 nm (Electro-Nucleonics) serving as column filling. After evaporation of the methanol, the polymer was redissolved in water.

**Characterization.** For our investigations we used the fraction with the highest molecular weight. The polymer concentrations of the fractionated methanolic solution and of the aqueous stock solution were determined by interferometric refractometry (Optilab 5902) at 25 °C, using  $0.164 \pm 0.003$  and  $0.162 \pm 0.003$  cm<sup>3</sup>/g for the refractive index increments of poly(NIPAM) in water and methanol, respectively. Molecular weight and second virial coefficient were obtained in aqueous solution at 25 °C: From a three-parameter fit of eq 4 to the intensity data in the angle range 25–70°, we have  $M_w = (7.0 \pm 0.5) \times 10^6$  and  $A_2 = (6.3 \pm 0.5) \times 10^{-5}$  (mol cm<sup>3</sup>)/g<sup>2</sup>, while  $R_g$  at this temperature amounts to  $135 \pm 5$  nm. The constants  $k_D$  was computed from concentration-dependent QLS data as  $487 \pm 70$  cm<sup>3</sup>/g. The polydispersity was estimated from QLS measurements in the globule state at the highest scattering angle, where dust effects may be neglected. From  $\langle D^2(M) \rangle_z / \langle D(M) \rangle_z^2 = 0.0256 \pm 0.0036$ , we calculated  $M_w/M_n = 1.31 \pm 0.06$ . This value can be regarded as an upper limit, since for narrow molecular weight distributions, the second cumulant is known to overestimate the polydispersity.<sup>30,31</sup>

**Sample Preparation.** Polymer and surfactant stock solutions were mixed with the solvent, dust-free reagent grade water from a Milli-Q apparatus. To control the ionic strength and to prevent bacteria growth, we added  $5 \times 10^{-4}$  mol/L  $NaNO_3$ . Precautions were taken to eliminate dust from the solutions: Upon mixing, surfactant stock solution and solvent were filtered with 20-nm membrane filters (Anotop). The polymer-surfactant solutions were again filtered prior to the experiment by means of 450-nm

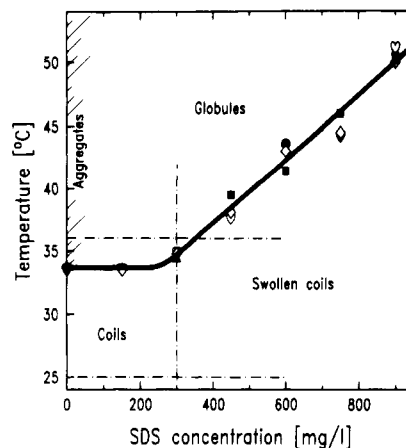


**Figure 1.** Phase diagram of poly(NIPAM) with temperature and SDS concentration as independent variables for various polymer concentrations: (●)  $c = 10$  mg/L; (■)  $c = 50$  mg/L; (▽)  $c = 100$  mg/L; (◇)  $c = 200$  mg/L; (▲) unfractionated sample from previous work,  $c = 100$  mg/L. Horizontal and vertical dashed lines refer to experiments shown in Figures 2 and 3, respectively.

membrane filters (Millipore-HV). To ensure reproducibility and to prevent shear-induced degradation of the polymer chains, this filtration process was carried out with an automatic syringe driver with a flow rate of only 0.2 mL/min.

The polymer concentration  $c_p$  was chosen to be 50 mg/L throughout the investigation (the determination of the phase behavior of the poly(NIPAM)-SDS system, however, was carried out at polymer concentrations ranging from 10 to 200 mg/L, as shown in Figure 1). The surfactant concentration was varied between 0 and 900 mg/L. With an overlap concentration  $c^* = (3M_w/4\pi N_A R_g^3)$  of 1.1 g/L for the polymer coils and with a critical micellization concentration of 2.3 g/L for SDS in water,<sup>32</sup> the solutions may be regarded as dilute with respect to both polymer and surfactant concentration.

**Light Scattering.** We use a modified spectrometer (ALV) for simultaneous static and dynamic light scattering experiments. To ensure directional stability of the incident light (the vertically polarized 514-nm line of an argon ion laser), the laser beam is guided by means of a polarization-preserving fiber with integrated optics (York). An automatic electrooptical coupling device (Launchmaster, York) ensures stability of the coupling efficiency. The temperature of the samples is controlled to 0.02 °C with an external heat bath (Lauda) and a calibrated Pt-100 temperature sensor. Prior to and after each experiment, toluene is used to check the adjustment of the apparatus and as a calibration standard for the determination of the Rayleigh ratios. The value for the Rayleigh ratio of toluene  $R_{90,0}$  for vertically polarized incident and scattered light at 25 °C and 514.5 nm was extrapolated from data at 488 nm<sup>33</sup> to  $(3.24 \pm 0.05) \times 10^{-6}$  cm<sup>-1</sup>. The angle range for intensity measurements was between 25 and 145°. The values of  $R_{\theta=0}$  could be determined to approximately 5%, and the radii of gyration to 2%. The transition temperatures were determined from the scattering intensities at the highest scattering angle of 145°, where the difference in scattering by coils and globules is most pronounced (see Figure 4). The sample was heated at a rate of 0.4 °C/h. No change of the results was observed when the heating rate was further lowered. QLS measurements were performed at angles between 25 and 48° using a 4-bit digital correlator with 136 channels (Brookhaven Instruments). The experimental error in the determination of  $R_h$  from eq 10 was 2%.

## Results and Discussion

In Figure 1, we show the phase behavior of the poly(NIPAM)-SDS system, i.e., the transition temperature  $T_c$  as a function of the surfactant concentration  $c_s$  for various polymer concentrations in the dilute regime.

The terms indicating different conformational states of the polymer will be motivated later, and we now proceed

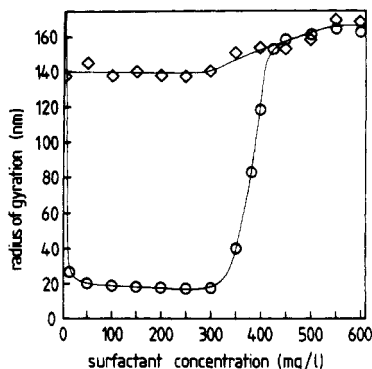


**Figure 2.** Radius of gyration as a function of surfactant concentration for temperatures below and above the LCST: ( $\diamond$ )  $T = 25\text{ }^{\circ}\text{C}$ ; ( $\circ$ )  $T = 36\text{ }^{\circ}\text{C}$ .

to discuss the transition behavior: For SDS concentrations up to approximately 300 mg/L,  $T_c$  remains constant and equals the LCST of  $34\text{ }^{\circ}\text{C}$ . Upon further increase of  $c_s$ ,  $T_c$  is successively elevated to about  $50\text{ }^{\circ}\text{C}$  at 900 mg/L. We interpret this increase of  $T_c$  above a certain threshold of  $c_s$  as an indicator for enhanced adsorption of the surfactant to the polymer in the vicinity of this surfactant concentration, corroborating the notion of a critical association concentration by Schild and Tirrell.<sup>21</sup> The elevation of the transition temperature thus presumably results from repulsive electrostatic interactions between the ionic heads of the adsorbed surfactant molecules, inhibiting the collapse of the polymer chains. From our data, we can only speculate whether the surfactant molecules are adsorbed individually or whether they are bound to the polymer in the form of micelles as has been suggested by the same authors and has been observed for other polymer-surfactant systems.<sup>34,35</sup> We find—in agreement with the results of Kubota et al.<sup>18</sup>—that for surfactant-free solutions, the transition region is quite narrow ( $<1\text{ }^{\circ}\text{C}$ ) compared to the polystyrene solution systems.<sup>36,37</sup> With increasing surfactant content, the transition becomes broader: The width of the transition region increases from approximately  $1.5\text{ }^{\circ}\text{C}$  for  $c_s = 150\text{ mg/L}$  to  $6 \pm 2\text{ }^{\circ}\text{C}$  at  $c_s = 900\text{ mg/L}$ . Within experimental error,  $T_c$  does not depend on the polymer concentration, at least for the relatively low concentrations used in our experiments. Furthermore, the data included from our previous study demonstrate that the transition temperature does not appreciably depend on molecular weight and polydispersity of the polymer sample. (This insensitivity of  $T_c$  to polymer concentration and molecular weight has been reported for surfactant-free poly(NIPAM) solutions.<sup>6,17</sup>) We therefore assume that the transition temperature is primarily determined by local interaction effects rather than by properties related to the nature of a polymer molecule as a large system (in the sense of statistical thermodynamics). However, the flexibility and the high molecular weight of our polymer chains allow large conformational changes to be triggered by small changes in the subtle balance between the repulsive forces of the adsorbed surfactant molecules and the attractive forces between the polymer segments as well as between the polymer and the hydrophobic tails of the surfactant. The extent of these conformational changes is shown in Figures 2 and 3, where the size of the polymer molecules is plotted as a function of surfactant concentration and temperature, respectively. First we discuss the effects of surfactant concentration, as shown in Figure 2 (and indicated by the horizontal dashed lines in Figure 1).

At  $25\text{ }^{\circ}\text{C}$ , well below the LCST, we observe an increase of the polymer size above a surfactant concentration in

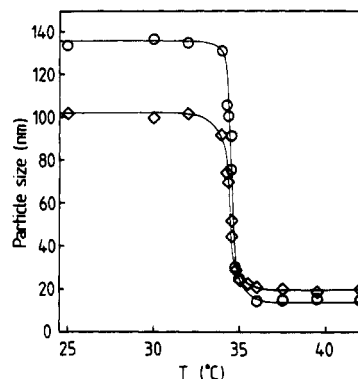


**Figure 3.** Hydrodynamic radius ( $\diamond$ ) and radius of gyration ( $\circ$ ) as a function of temperature. Surfactant concentration is 300 mg/L.

the vicinity of 300 mg/L. We interpret this swelling as another indicator for the cooperative binding of surfactant to the polymer chain resulting in an expansion of the chains due to the repulsive interactions between the firmly adsorbed amphiphiles. However, the swelling of the polymer coils with increasing surfactant concentration is rather moderate, because, due to its stiffness, poly(NIPAM) in water adopts a rather expanded conformation even in the absence of surfactant.<sup>14</sup> Also interesting is the behavior of  $R_{\theta=0}$ , i.e., of the apparent molecular weight (not shown in the figure): It increases first sharply to reach the value of  $23.6 \times 10^{-5}\text{ cm}^{-1}$  already at  $c_s = 50\text{ mg/L}$ , which amounts to a 40% increase compared to the surfactant-free polymer solution. With further increase of surfactant content, however,  $R_{\theta=0}$  decreases gradually to reach again the surfactant-free value at  $c_s = 500\text{ mg/L}$ . At the present stage, we can interpret these observations only qualitatively. We presume that this phenomenon is very similar to the preferential solvation observed with polymers in binary solvents.<sup>38,39</sup> At small surfactant concentrations, the interior of the coils is enriched by surfactant. However, the gradient between the interior of the coils and the surrounding solution decreases upon further addition of surfactant and therefore the scattering intensity decreases. It appears that at small concentrations of surfactant, the binding of surfactant molecules to the polymer is too weak to influence the polymer conformation. Above 300 mg/L, however, the binding is stabilized by cooperative effects, and this leads to swelling of the coils. Above the LCST, at  $36\text{ }^{\circ}\text{C}$ , the conformation strongly depends on the surfactant concentration: Without surfactant, we observe large aggregates. Already 10 mg/L SDS is sufficient to greatly reduce the aggregation. Though the size of the scattering particles decreases well below the size of the coil state, there are still aggregates present. The number of macromolecules incorporated into an aggregate, however, decreases upon further increase in surfactant concentration. The mean aggregation number can be determined quantitatively by comparing the scattering intensities at zero scattering angle below and above the transition: The ratio  $R_{\theta=0}(T=36)/R_{\theta=0}(T=25)$  and thus the aggregation number decrease with increasing surfactant concentration from a value of  $\approx 6$  for  $c_s = 10\text{ mg/L}$  to unity at 250 mg/L, where the intermolecular solubilization is completed. (The apparent molecular weight of the completely solubilized globules is, however, increased by the adsorbed surfactant to the same extent as for coils at  $25\text{ }^{\circ}\text{C}$ .) This decrease of the aggregation number is also reflected by the decrease of  $R_g$  from 25 nm at  $c_s = 10\text{ mg/L}$  to 16 nm for  $c_s = 250\text{ mg/L}$ . These observations clearly demonstrate the existence of isolated collapsed polymer chains. Note that in this state, the

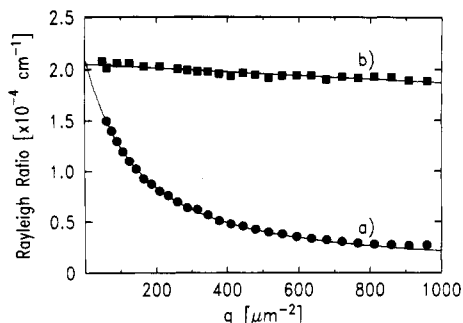


**Figure 4.** Angle dependency of Rayleigh ratio below and above the LCST, reflecting (a) the extended coil state at  $T = 25\text{ }^{\circ}\text{C}$  and (b) the collapsed globule state at  $T = 36\text{ }^{\circ}\text{C}$ . Note that the data have not been normalized; the congruency of the y-axis intercepts thus demonstrates the absence of aggregates. For data set (a) we show the fit of eq 5 in the angle range  $25\text{--}70^{\circ}$ ; for data set (b) the line is the fit of eq 6 in the whole angle range. Surfactant concentration is 250 mg/L.

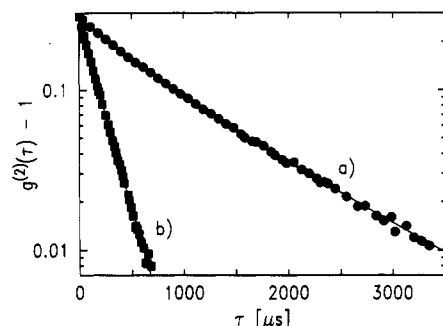


**Figure 5.** Correlation functions below and above the LCST: (a)  $T = 25\text{ }^{\circ}\text{C}$  (coils); (b)  $T = 36\text{ }^{\circ}\text{C}$  (globules). The lines represent four-parameter cumulant fits. Surfactant concentration is 250 mg/L.

suspension remained stable during the observation time of several weeks. We postpone the analysis of the nature of the collapsed state to the discussion of Figure 3 and consider first another interesting feature of the polymer-surfactant solutions: With further increasing surfactant concentration, we observe intramolecular solubilization: the collapsed polymer molecules expand again, and the radius of gyration eventually reaches the same value as below the LCST. The repulsive forces of the adsorbed surfactant apparently become strong enough to overcome the attraction between the polymer segments at the given temperature. (However, the polymer collapses when the temperature is elevated to the  $T_c$  corresponding to the surfactant concentration (recall Figure 1).) The location and the width of this transition compare well with the results from our first investigation on the unfractionated sample.<sup>6</sup>

We now fix the surfactant concentration at 300 mg/L and vary the temperature (following the vertical dashed line in Figure 1), obtaining the data on the radius of gyration and the hydrodynamic radius shown in Figure 3.

Below the transition temperature, both the geometric and hydrodynamic sizes are constant; the ratio  $R_g/R_h$  is  $1.34 \pm 0.04$ , reflecting the coil state of the polymer: This value for  $R_g/R_h$  lies within the range 1.24–1.56 predicted by renormalization group theory in the nondraining limit for Gaussian and self-avoiding chains, respectively,<sup>40</sup> but it is lower than the 1.50 resulting from the Kirkwood-Riseman approach for Gaussian coils in the same limit.<sup>23</sup> The particle scattering factors and the correlation functions correspond to curves (a) in Figures 4 and 5. At  $34.8\text{ }^{\circ}\text{C}$ , the chains collapse. (In the vicinity of the transition region, the shape of the particle scattering factors and the

correlation functions suggest the coexistence of globules and coils or partially collapsed chains.) The width of this region is somewhat less than  $1\text{ }^{\circ}\text{C}$ , as in our previous study. The hydrodynamic radius drops from  $101 \pm 2\text{ nm}$  to  $19.8 \pm 0.8\text{ nm}$ , and the radius of gyration from  $135 \pm 3\text{ nm}$  to  $16.0 \pm 0.5\text{ nm}$ , reflecting a reduction of the volume occupied by the polymer chain by a factor of more than 300. In the collapsed regime beyond the transition temperature, both sizes are again constant. The particle scattering factors and correlation functions are of the shape (b) in the corresponding Figures 4 and 5.

In this regime, the radius of gyration is smaller than the hydrodynamic radius, which is consistent with the picture of compact globules. Moreover, the experimental value of  $0.81 \pm 0.06$  for  $R_g/R_h$  is in very good agreement with the theoretical one of  $(3/5)^{1/2}$  for a homogeneous sphere impermeable to the solvent. The density of the globules, calculated from the hydrodynamic radius to be  $0.36 \pm 0.03\text{ g/cm}^3$ , agrees very well with the  $0.40 \pm 0.04\text{ g/cm}^3$  we were able to realize with a space-filling model of the polymer and with the value of  $0.32 \pm 0.04\text{ g/cm}^3$  measured on collapsed poly(NIPAM) gels.<sup>41</sup> The high density of the polymeric material in collapsed globules also accounts for our observation of vanishing mobility of polymer-bound fluorescent probes.<sup>20</sup>

## Conclusions

Our study of the phase behavior of a monodisperse, high molecular weight sample of poly(NIPAM) in aqueous solution by static and quasielastic light scattering leads to the following conclusions: As indicated in our first report, intermolecular solubilization by small amounts of surfactant completely prevents aggregation of the collapsed macromolecules at temperatures above the LCST. This allows the investigation of isolated polymer molecules in the whole temperature range and the observation of their temperature-induced conformational transition, which would otherwise be masked by aggregation. The value of the transition temperature and the width of the transition region do not depend appreciably on polymer concentration, polydispersity, and molecular weight of the sample, indicating that the transition is governed by local, short-range interaction effects. During this transition, the geometric size of the polymer molecules changes from 135 to 20 nm, equaling a reduction of the polymer volume by a factor of more than 300. In the collapsed state, the ratio  $R_g/R_h = 0.81$  and the high density of  $0.36\text{ g/cm}^3$  are characteristic for impermeable spheres. We conclude thus: The temperature-induced conformational transition of poly(NIPAM) is the long-pursued coil-to-globule transition: Above  $T_c$  we have a stable suspension of isolated (solubilized) polymeric globules.

Following an isotherm at a sufficiently high temperature, we observe a new phenomenon, i.e., the intramolecular solubilization which manifests itself as a surfactant-induced globule-to-coil transition. The microscopic mechanism of the intramolecular solubilization remains to be elucidated. There are, however, clues that the transition is governed by cooperative binding of the surfactant to the polymer: The surfactant affects also the coil state below the LCST. We observe a swelling of the coils which sets on at 300 mg/L in coincidence with the upturn of the transition temperature  $T_c$ . This critical value of surfactant concentration is close to the critical association concentration of 230 mg/L determined by Schild and Tirrell,<sup>21</sup> who conclude from their study that the surfactant is adsorbed cooperatively in the form of micelles. At the present stage of investigation, the discussion has

to remain somewhat speculative, because the amounts of surfactant loosely associated with the polymer molecules or firmly and cooperatively bound to the chain remain yet to be determined. This task is not easy, but its accomplishment is crucial for the understanding of the intriguing phenomena resulting from the interaction of surfactants with the thermosensitive polymer.

**Acknowledgment.** This research has been supported by the Swiss National Science Foundation.

## References and Notes

- (1) Lindmann, B.; Karlström, G. *Z. Phys. N.F.* **1987**, *155*, 199.
- (2) Chu, B.; Xu, R.; Wang, Z.; Zuo, J. *J. Appl. Crystallogr.* **1988**, *21*, 707 and references cited therein.
- (3) Park, I. H.; Wang, Q. W.; Chu, B. *Macromolecules* **1987**, *20*, 1965.
- (4) Goddard, E. D. *Colloids Surf.* **1986**, *19*, 255.
- (5) Lin, T. H.; Leed, A. R.; Scheraga, H. A.; Mattice, W. L. *Macromolecules* **1988**, *21*, 2447 and references cited therein.
- (6) Rička, J.; Meewes, M.; Nyffenegger, R.; Binkert, Th. *Phys. Rev. Lett.* **1990**, *65*, 657.
- (7) Heskins, M.; Guillet, J. E. *J. Macromol. Sci.* **1968**, *A2(8)*, 1441.
- (8) Agency of Industrial Sciences and Technology of Japan, Patent No. 83 78580 Cl:B32B27/30, 1983.
- (9) Agency of Industrial Sciences and Technology of Japan, Patent No. 95930 Cl:B01J20/26, 1984.
- (10) Okahata, Y. *Macromolecules* **1986**, *19*, 493.
- (11) Dong, L. C.; Hoffman, A. S. In *Reversible Polymer Gels and Related Systems*; Russo, P. S., Ed.; American Chemical Society: Washington, DC, 1987; Chapter 16.
- (12) Cole, C.; Schreiner, S.; Priest, J.; Monji, N.; Hoffman, A. S. In *Reversible Polymer Gels and Related Systems*; Russo, P. S., Ed.; American Chemical Society: Washington, DC, 1987; Chapter 17.
- (13) Hirokawa, Y.; Tanaka, T. *J. Chem. Phys.* **1984**, *81*, 6379.
- (14) Fujishige, S. *Polym. J.* **1987**, *19*, 297.
- (15) Winnik, F. M. *Polymer* **1990**, *31*, 2125.
- (16) Winnik, F. M. *Macromolecules* **1990**, *23*, 233.
- (17) Fujishige, S. *J. Phys. Chem.* **1989**, *93*, 3311.
- (18) Kubota, K.; Fujishige, S.; Ando, I. *J. Phys. Chem.* **1990**, *94*, 5154.
- (19) Yamamoto, I.; Iwasaki, K.; Hirotsu, S. *J. Phys. Soc. Jpn.* **1989**, *58*, 210.
- (20) Binkert, Th.; Oberreich, J.; Meewes, M.; Nyffenegger, R.; Rička, J. *Macromolecules* **1991**, *24*, 5806.
- (21) Schild, H. G.; Tirrell, D. A. *Polym. Prepr. (Am. Chem. Soc., Div. Polym. Chem.)* **1989**, *30(2)*, 350.
- (22) Bantle, S.; Schmidt, M.; Burchard, W. *Macromolecules* **1982**, *15*, 1604.
- (23) Yamakawa, H. *Modern Theory of Polymer Solutions*; Harper and Row: New York, 1971.
- (24) Zimm, B. H. *J. Chem. Phys.* **1948**, *16*, 1099.
- (25) Debye, P. *J. Phys. Colloid Chem.* **1947**, *51*, 18.
- (26) Mattice, W. L. *Macromolecules* **1982**, *15*, 579.
- (27) Kerker, M. *The Scattering of Light and Other Electromagnetic Radiation*; Academic Press: New York, 1969.
- (28) Berne, B.; Pecora, R. *Dynamic Light Scattering*; Wiley and Sons: New York, 1976.
- (29) Kulicke, W.; Klein, J. *Angew. Makromol. Chem.* **1987**, *69*, 169.
- (30) Candau, S. J. In *Scientific Methods for the Study of Polymer Colloids and Their Applications*; Candau, F., Ottewill, R. H., Eds.; Kluwer Academic Publishers: Dordrecht, Holland, 1990; p 329.
- (31) Schurtenberger, P. Institute for Polymer Research, ETH Zürich, Switzerland, unpublished.
- (32) Hunter, R. *Foundations of Colloid Science*; Clarendon: Oxford, 1987; Chapter 10.
- (33) Bender, Th.; Lewis, R. J.; Pecora, R. *Macromolecules* **1986**, *19*, 244.
- (34) Cabane, B.; Duplessix, R. *J. Phys. (Paris)* **1982**, *43*, 1529.
- (35) Quina, F.; Abuin, E.; Lissi, E. *Macromolecules* **1990**, *23*, 5173.
- (36) Vidakovic, P.; Rondelez, F. *Macromolecules* **1984**, *17*, 418.
- (37) Chu, B.; Park, I. H.; Wang, Q. W.; Wu, C. *Macromolecules* **1987**, *20*, 2833.
- (38) Kratochvil, P.; Sundelöf, L.-O. *Acta Pharm. Suec.* **1986**, *23*, 31.
- (39) Stejskal, J.; Kratochvil, P. *J. Polym. Sci., Polym. Phys. Ed.* **1975**, *13*, 715.
- (40) Oono, Y.; Kohmoto, M. *J. Chem. Phys.* **1983**, *78(1)*, 520.
- (41) Marchetti, M.; Prager, S.; Cussler, E. L. *Macromolecules* **1990**, *23*, 3445.

**Registry No.** Poly(NIPAM), 25189-55-3; SDS, 151-21-3.